Electronic Supplementary Material (ESI) for Analyst.

Supporting Information

Simultaneous and Site-specific Profiling of Heterogeneity and Turnover in Protein S-acylation by Intact S-acylated Peptides Analysis with a Cleavable Bioorthogonal Tag

Roujun Wu,[a] Guanghui Ji,[a] Weiyu Chen,[a] Lei Zhang,[b] Caiyun Fang,*[a] Haojie Lu*[ab]

[a] Department of Chemistry and Liver Cancer Institute, Zhongshan Hospital, Fudan University, Shanghai 200433, P. R. China.

[b] Institutes of Biomedical Sciences and NHC Key Laboratory of Glycoconjugates Research, Fudan University, Shanghai 200032, P. R. China.

*Email: C.F. (fangcaiyun@fudan.edu.cn); H.L. (luhaojie@fudan.edu.cn)

Supplementary Figures

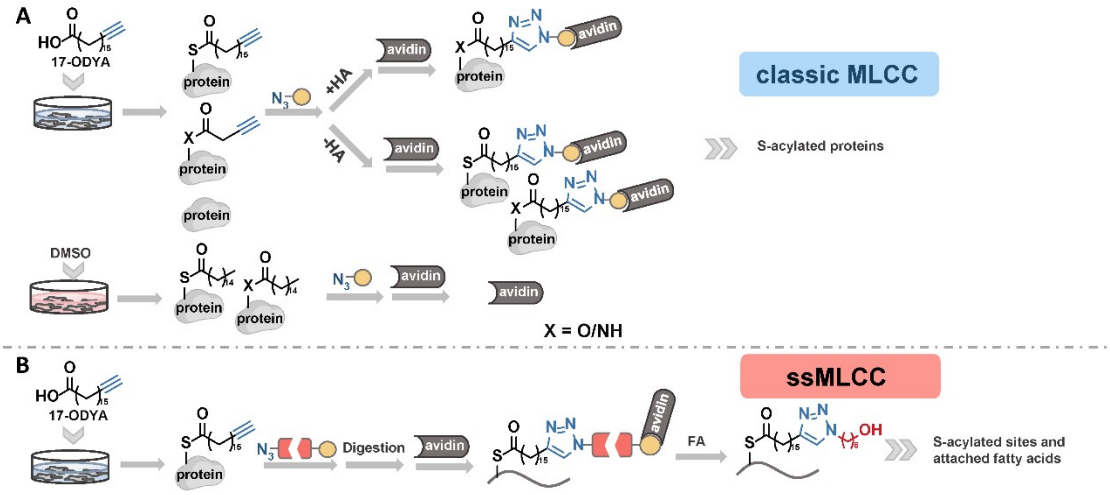

Fig. S1 Comparison classic MLCC and ssMLCC. (A) Classic MLCC studies can only identify S-acylated proteins and require two control groups, one is DMSO-labelled group to distinguished non-specific absorption, the other is HA treatment group to exclude other types of acylated protein (*e.g.*, N- and O- acylation). Moreover, the exact form of S-acylation could not be distinguished. (B) In ssMLCC, intact S-acylated peptides were obtained, contributing to precise mapping of S-acylated sites with attached fatty acids.

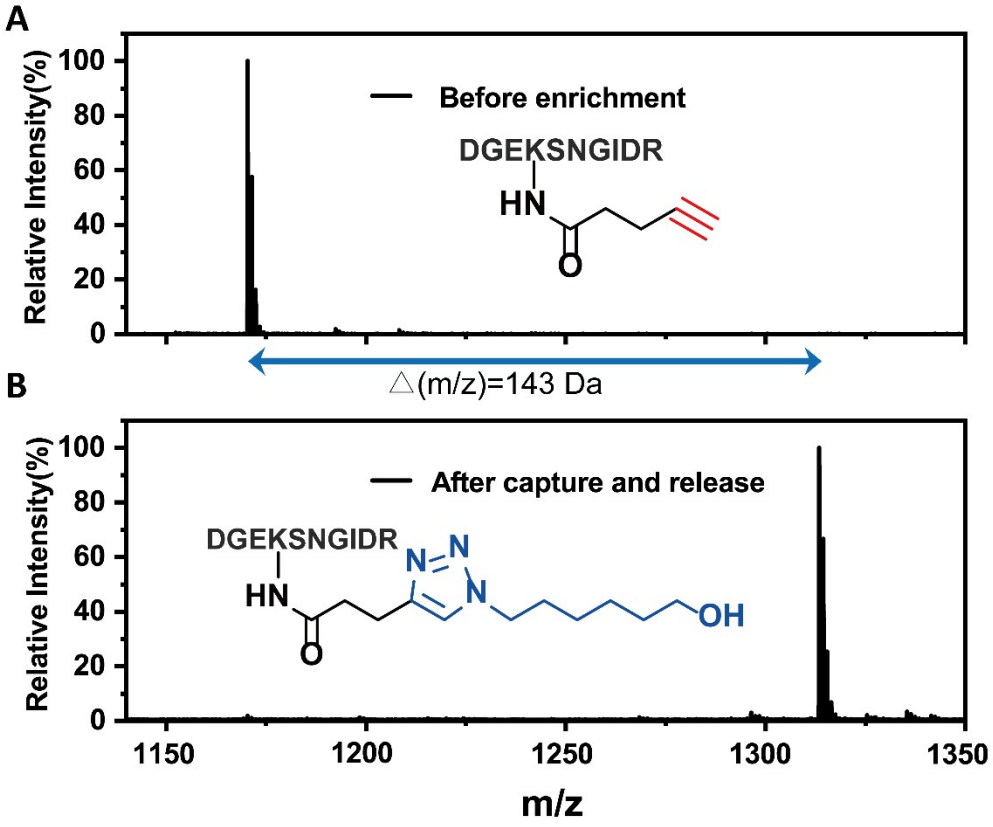

Fig. S2 Alkynyl peptides (DGEK$^{\text{pentinoic acid}}$SNGIDR) was conjugated with DADPS biotin through CuAAC reaction, captured by avidin beads and released by 10% FA. (A) MALDI-TOF MS analysis result of the alkynyl peptides before enrichment, and (B) MALDI-TOF MS analysis result of the recovered peptides after capture and release, with an additional tag of 143 Da.

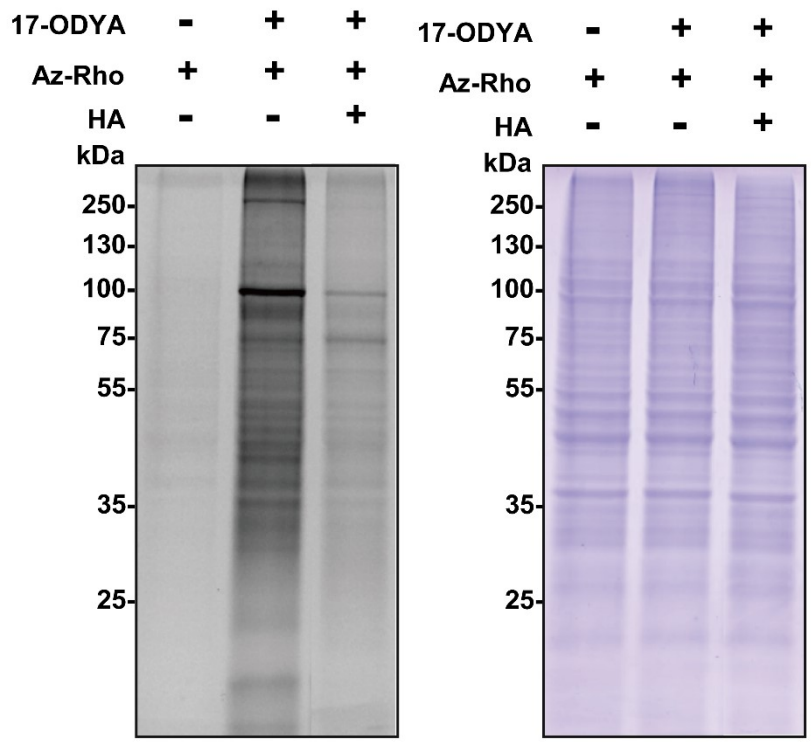

Fig. S3 Labelling efficiency of 17-ODYA in HeLa cells. HeLa cells were metabolically labelled with 17-ODYA and lysed. Then 17-ODYA-labelled proteins were conjugated with fluorescent probe (5-TAMRA azide) through CuAAC reaction, separated by SDS-PAGE and visualized by in-gel fluorescence. To distinguish hydroxylamine-sensitive 17-ODYA-labelled proteins, proteins were treated with neutral hydroxylamine before being diluted with loading buffer. The left picture referred to in-gel fluorescence result and the right one was the Coomassie staining result.

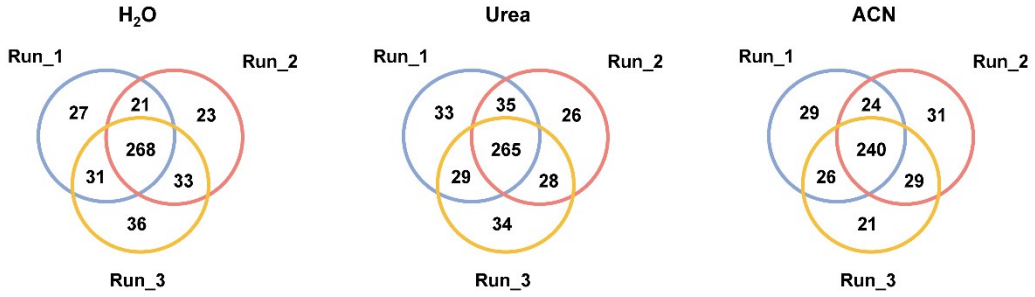

Fig. S4 Overlap of the S-palmitoylated peptides (AScore≥19) identified among three replicates in three release condition experiments.

Peptide	-10LgP	m/z	AScore	Accession
SGGC(+405.34)GVSAGNGK	75.02	699.8912	1001	Q9NV58

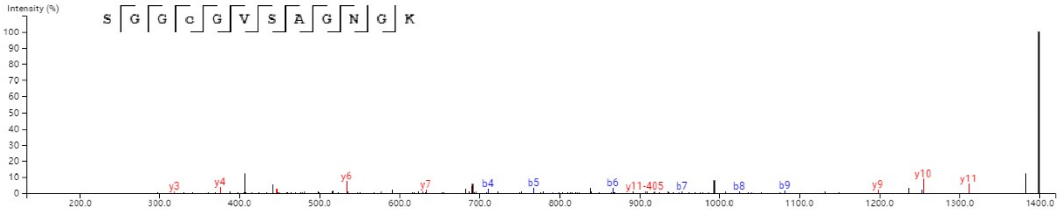

#	b	b-Neutral Loss	b(2+)	Seq	y	y-Neutral Loss	y(2+)	#
1	88.04		44.52	S				12
2	145.06		73.03	G	1311.73	906.40	656.37	11
3	202.08		101.54	G	1254.71	849.39	627.86	10
4	710.42	305.09	355.71	C(+405.34)	1197.69	792.37	599.35	9
5	767.45	362.11	384.22	G	689.36		345.18	8
6	866.52	461.18	433.76	V	632.33		316.67	7
7	953.55	548.21	477.27	S	533.27		267.13	6
8	1024.57	619.25	512.79	A	446.23		223.62	5
9	1081.60	676.27	541.30	G	375.20		188.10	4
10	1195.66	790.32	598.33	N	318.17		159.59	3
11	1252.66	847.33	626.84	G	204.13		102.57	2
12				K	147.11		74.06	1

Fig. S5 Mass spectrum of C460 in RNF19A to be identified as a novel S-palmitoylated site. RNF19A is predicted to be S-acylated in Swisspalm but first to be identified in palmitoyl proteomics studies by our ssMLCC method. Here, the palmitoyl loss together with its additional mass tag was observed in CID mode of timsTOF Pro mass spectrometer, represented by 'Neutral Loss' in this figure.

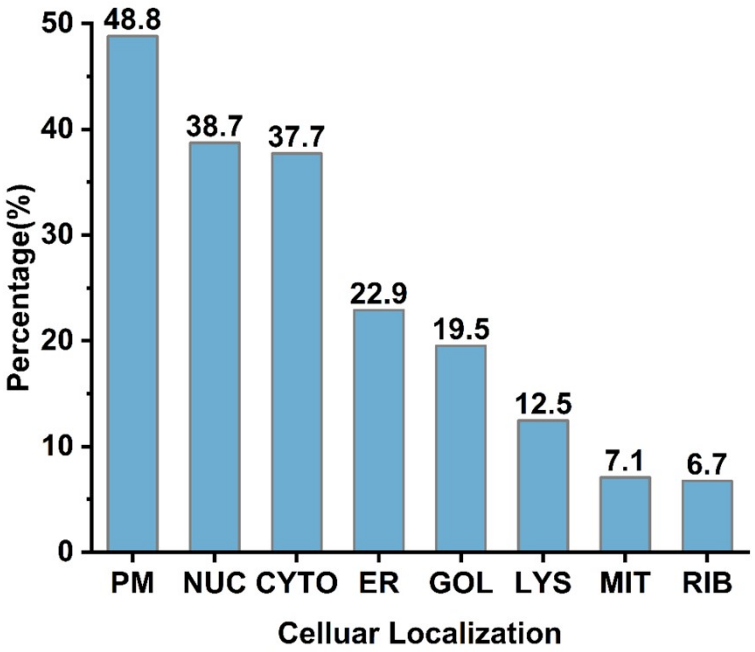

Fig. S6 Gene ontology cellular localization analysis of 297 candidate S-palmitoylated proteins. PM-plasma membrane; NUC-nucleus; CYTO-cytosol; ER-endoplasmic reticulum; GOL-Golgi apparatus; MIT-mitochondria; LYS-lysosome; RIB-ribosome. The overall proportion was over 100 because some proteins located in more than one cellular compartments.

Peptide	-10LgP	m/z	AScore	Accession
MFFTC(+125.05)GPNEAMVVSGFC(+405.34)R	94.43	842.7506	126.6920	O75955

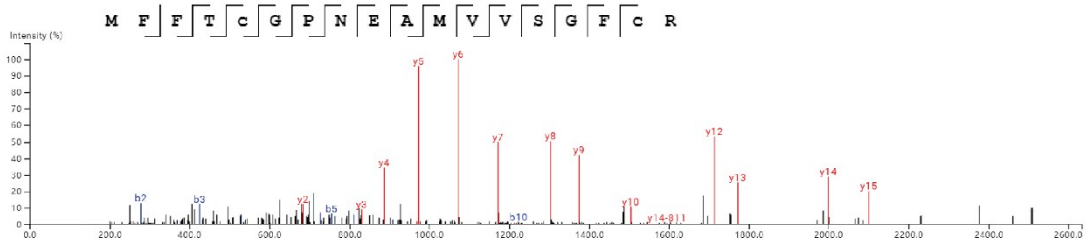

#	b	b-Neutral Loss	b(2+)	Seq	y	y-Neutral Loss	y(2+)	#
1	132.05		66.52	M				18
2	279.11		140.06	F	2395.20	1989.87	1198.10	17
3	426.18		213.59	F	2248.13	1842.80	1124.57	16
4	527.23		264.12	T	2101.04	1695.73	1051.03	15
5	755.29		378.17	C(+125.05)	2000.01	1594.67	1000.51	14
6	812.32		406.66	G	1771.95	1366.62	886.48	13
7	909.35		455.18	P	1714.94	1309.60	857.97	12
8	1023.41		512.20	N	1617.89	1212.52	809.44	11
9	1152.45		576.72	E	1503.85	1098.51	752.42	10
10	1223.51		612.24	A	1374.81	969.42	687.90	9
11	1354.53		677.76	M	1303.77	898.43	652.38	8
12	1453.60		727.28	V	1172.72	767.39	586.86	7
13	1552.66		776.83	V	1073.65	668.32	537.33	6
14	1639.70		820.35	S	974.58	569.25	487.79	5
15	1696.72		848.86	G	887.53	482.22	444.28	4
16	1843.79		922.39	F	830.53	425.18	415.77	3
17	2352.13	1946.79	1176.57	C(+405.34)	683.45	278.13	342.23	2
18				R	175.12		88.06	1

Fig. S7 Mass spectrum of C17 in FLOT1 to be identified as a novel S-palmitoylated site.

Peptide	-10LgP	m/z	AScore	Accession
IQGQNKEMLAAAC(+405.34)QMFLGKTEAEIA HIALETLEGHQR	61.32	897.8793	1001	O75955

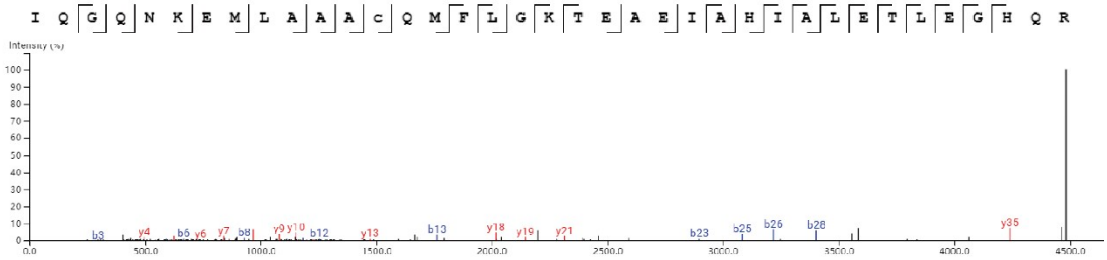

#	b	b-Neutral Loss	b(2+)	Seq	y	y-Neutral Loss	y(2+)	#
1	114.09		57.55	I				37
2	242.15		121.58	Q	4372.30	3966.96	2186.65	36
3	299.16		150.09	G	4244.21	3838.90	2122.62	35
4	427.23		214.12	Q	4187.22	3781.88	2094.11	34
5	541.27		271.14	N	4059.16	3653.82	2030.08	33
6	669.36		335.18	K	3945.12	3539.78	1973.06	32
7	798.41		399.71	E	3817.02	3411.69	1909.01	31
8	929.44		465.23	M	3687.98	3282.64	1844.49	30
9	1042.54		521.77	L	3556.94	3151.60	1778.97	29
10	1113.56		557.29	A	3443.85	3038.52	1722.43	28
11	1184.61		592.81	A	3372.82	2967.48	1686.91	27
12	1255.62		628.32	A	3301.78	2896.44	1651.39	26
13	1764.01	1358.66	882.50	C(+405.34)	3230.74	2825.41	1615.87	25
14	1892.05	1486.71	946.53	Q	2722.40		1361.70	24
15	2023.07	1617.76	1012.05	M	2594.34		1297.67	23
16	2170.16	1764.82	1085.58	F	2463.30		1232.15	22
17	2283.26	1877.91	1142.12	L	2316.25		1158.62	21
18	2340.26	1934.93	1170.63	G	2203.15		1102.07	20
19	2468.36	2063.02	1234.68	K	2146.10		1073.56	19
20	2569.41	2164.07	1285.20	T	2018.02		1009.52	18
21	2698.45	2293.11	1349.77	E	1916.98		958.99	17
22	2769.49	2364.15	1385.24	A	1787.94		894.47	16
23	2898.51	2493.19	1449.76	E	1716.90		858.95	15
24	3011.61	2606.28	1506.31	I	1587.86		794.43	14
25	3082.62	2677.32	1541.83	A	1474.82		737.89	13
26	3219.68	2814.37	1610.35	H	1403.74		702.37	12
27	3332.79	2927.46	1666.90	I	1266.68		633.84	11
28	3403.80	2998.50	1702.42	A	1153.59		577.30	10
29	3516.91	3111.58	1758.96	L	1082.56		541.78	9
30	3645.96	3240.62	1823.48	E	969.47		485.24	8
31	3747.01	3341.67	1874.00	T	840.43		420.74	7
32	3860.09	3454.75	1930.54	L	739.38		370.19	6
33	3989.13	3583.80	1995.07	E	626.30		313.65	5
34	4046.15	3640.82	2023.58	G	497.25		249.13	4
35	4183.21	3777.88	2092.11	H	440.23		220.62	3
36	4311.27	3905.94	2156.14	Q	303.18		152.09	2
37				R	175.12		88.06	1

Fig. S8 Mass spectrum of C85 in FLOT1 to be identified as a novel S-palmitoylated site.

Peptide	-10LgP	m/z	AScore	Accession
VFVLPC(+405.34)IQQIQR	76.80	925.0813	1001	O75955

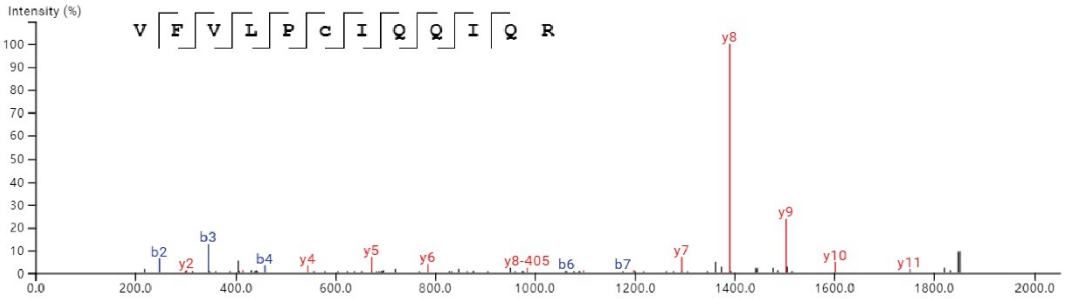

#	b	b-Neutral Loss	b(2+)	Seq	y	y-Neutral Loss	y(2+)	#
1	100.08		50.54	V				12
2	247.14		124.07	F	1750.09	1344.74	875.54	11
3	346.21		173.61	V	1603.01	1197.68	802.01	10
4	459.30		230.15	L	1503.93	1098.61	752.47	9
5	556.34		278.67	P	1390.86	985.52	695.93	8
6	1064.67	659.36	532.85	C(+405.34)	1293.81	888.46	647.40	7
7	1177.74	772.44	589.39	I	785.46		393.25	6
8	1305.83	900.50	653.42	Q	672.38		336.69	5
9	1433.91	1028.56	717.45	Q	544.32		272.66	4
10	1546.98	1141.64	773.99	I	416.26		208.63	3
11	1675.04	1269.70	838.02	Q	303.17		152.09	2
12				R	175.12		88.06	1

Fig. S9. Mass spectrum of C34 in FLOT1 to be identified as a S-palmitoylated site.

Peptide	-10LgP	m/z	AScore	Accession
NC(+405.34)MTDLLAK	48.25	707.4110	1001	Q00765

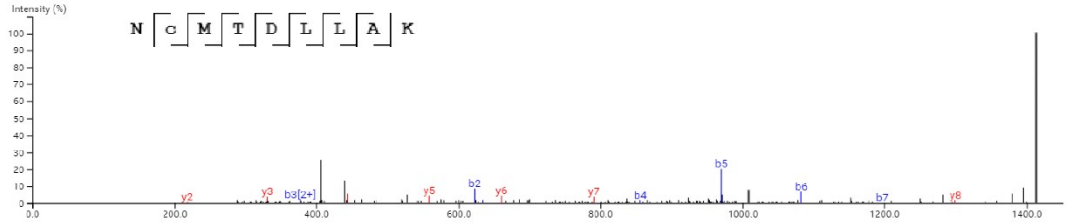

#	b	b-Neutral Loss	b(2+)	Seq	y	y-Neutral Loss	y(2+)	#
1	115.05		58.03	N				9
2	623.39	218.06	312.20	C(+405.34)	1299.79	894.44	650.39	8
3	754.44	349.10	377.72	M	791.43		396.22	7
4	855.48	450.15	428.24	T	660.39		330.70	6
5	970.52	565.18	485.76	D	559.34		280.16	5
6	1083.59	678.26	542.30	L	444.32		222.66	4
7	1196.69	791.33	598.84	L	331.23		166.12	3
8	1267.72	862.38	634.35	A	218.15		109.57	2
9				K	147.11		74.06	1

Fig. S10. Mass spectrum of C18 in REEP5 to be identified as a novel S-palmitoylated site.

Peptide	-10LgP	m/z	AScore	Accession
INRSPMC(+377.30)EYMINFIHKLK	85.93	872.1514	1001	P28347
INRSPMC(+403.32)EYMINFIHKLK	85.04	880.8282	1001	P28347
INRSPMC(+405.34)EYMINFIHKLK	74.89	881.4955	1001	P28347

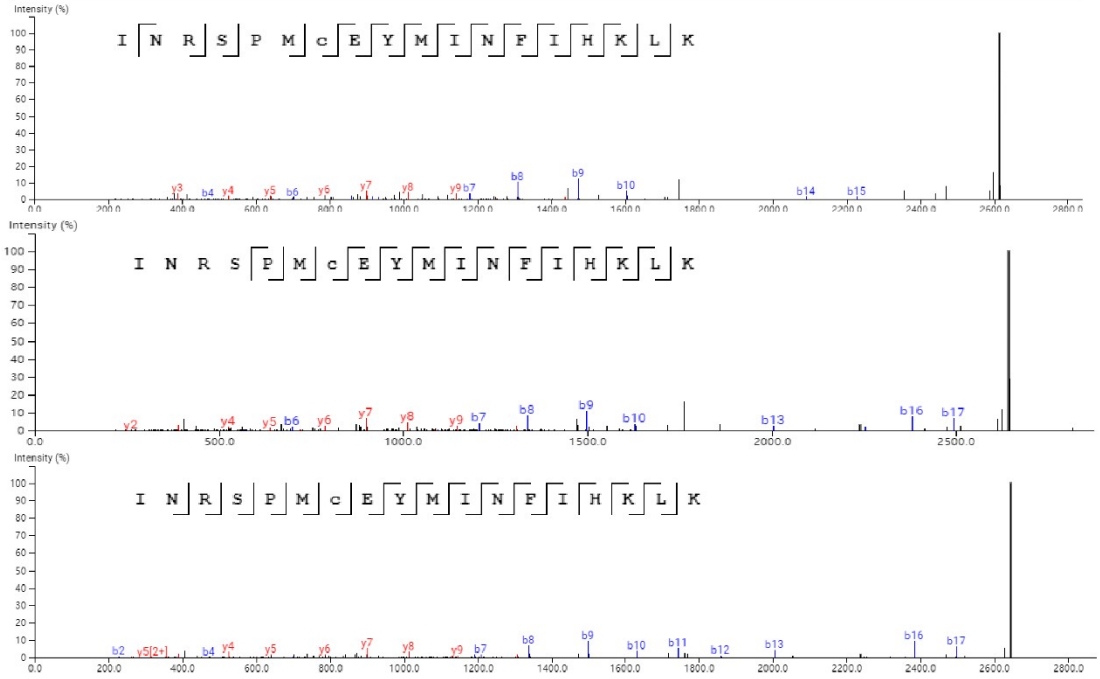

#	b	b(2+)	Seq	y	y(2+)	#
1	114.09;114.09;114.09	57.55;57.55;57.55	I			18
2	228.13;228.13;228.14	114.57;114.57;114.57	N	2501.36;2527.38;2529.39	1251.18;1264.19;1265.20	17
3	384.23;384.24;384.23	192.62;192.62;192.62	R	2387.32;2413.33;2415.35	1194.161207.17;1208.17	16
4	471.25;471.27;471.25	236.13;236.13;236.13	S	2231.22;2257.23;2259.25	1116.111129.12;1130.12	15
5	568.32;568.34;568.32	284.66;284.66;184.66	P	2144.18;2170.20;2172.21	1072.59;1085.60;1086.61	14
6	699.35;699.36;699.35	350.18;350.15;350.13	M	2047.13;2073.15;2075.16	1024.07;1037.07;1038.08	13
7	1179.67;1205.71;1207.70	590.34;603.35;604.35	C	1916.09;1942.11;1944.12	958.54;971.55;972.56	12
8	1308.70;1334.72;1336.74	654.86;667.87;668.87	E	1435.761435.78;1435.78	718.39;718.39;718.39	11
9	1471.78;1497.79;1499.81	736.39;749.40;750.41	Y	1306.73;1306.74;1306.74	653.87;653.87;653.87	10
10	1602.81;1628.83;1630.88	801.91;814.92;815.93	M	1143.67;1143.67;1143.66	572.34572.34;572.34	9
11	1715.91;1741.92;1743.97	858.45;871.46;872.47	I	1012.63;1012.63;1012.63	506.82;506.82;506.82	8
12	1829.95;1855.96;1857.95	915.47;928.48;929.49	N	899.54;899.54;899.54	450.28;450.27;450.27	7
13	1977.02;2003.04;2005.04	989.01;1002.02;1003.02	F	785.49;785.51;785.49	393.25;393.25;393.69	6
14	2090.06;2116.12;2118.13	1045.55;1058.56;1059.57	I	638.44;638.42;638.43	319.72319.72;319.69	5
15	2227.13;2253.18;2255.19	1114.08;1127.009;1128.10	H	525.35;525.34;525.35	263.18;263.18;263.18	4
16	2355.25;2381.30;2383.29	1178.14;1191.14;1192.14	K	388.29;388.29;388.29	194.65;194.65;194.65	3
17	2468.34;2494.34;2496.36	1234.63;1247.68;1248.68	L	260.20;260.21;260.19	130.60;130.60;130.60	2
18			K	147.11;147.11;147.11	74.06;74.06;74.06	1

Fig. S11. Mass spectra of C359 in TEAD1 to be modified with alk-C14:0, alk-C16:0 and alk-C16:1 by open search. Three figures in the second, third, fifth and sixth column referred to the messages about the above first, second, and third spectrum, respectively.

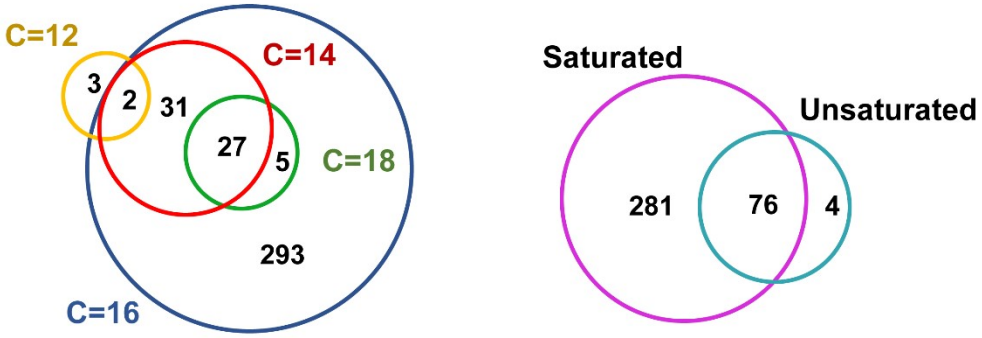

Fig. S12 Overlap of site-specific S-acylation heterogeneity in terms of chain length (left) and saturation (right).

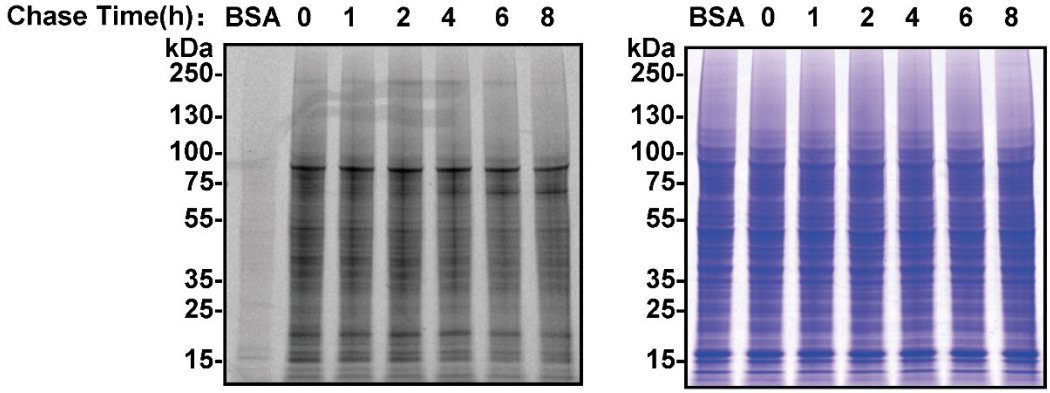

Fig. S13 In-gel fluorescence results of pulse-chase experiments. HeLa cells were pulsed with 17-ODYA for 2 h, following by being chased with excess palmitic acid for varying time points. Cells were harvested, lysed and then 17-ODYA labelled proteins were conjugated with 5-TAMRA azide through CuAAC reaction, separated by SDS-PAGE and visualized by in-gel fluorescence. The left picture referred to in-gel fluorescence result and the right one was the Coomassie staining result.

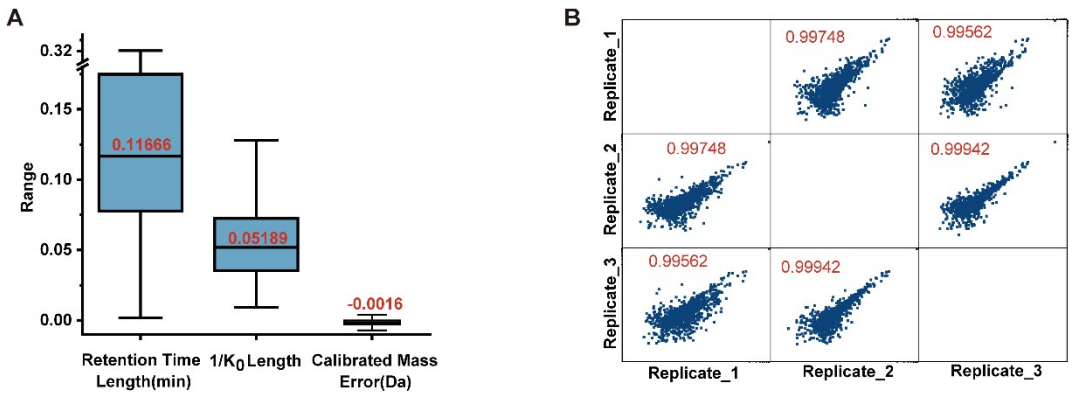

Fig. S14 (A) Box plots of retention time length, $1/K_0$ length and calibrated mass error of matched features in label-free quantification results. (B) Multi scatter plots the non-imputed LFQ values for each replicate two by two when chasing for 0 h (n=3).

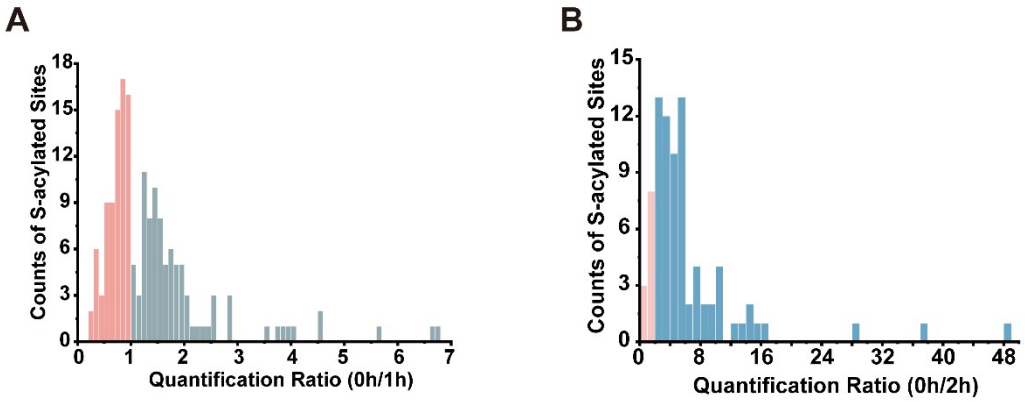

Fig. S15 (A) Histogram display of quantification ratio between two chase experiments (0 h/1 h). The pink bars referred to those sites with increasing 17-ODYA-labelled signals when chased for 1h. (B) Histogram display of quantification ratio between two chase experiments (0 h/2 h). The blue bars referred those rapid-cycling sites decreased with more than two-fold in 17-ODYA-labelled signals when chased for 2h.

Fig. S16 Motif analysis of peptide sequences adjacent with modified cysteine using pLogo. ‘Fg’ in the figure referred to S-palmitoylation proteins and ‘bg’ referred to human proteins.